

Uniform volume heating of mixed fuels within the ICF paradigm

Hartmut Ruhl and Georg Korn

Marvel Fusion, Theresienhöhe 12, 80339 Munich, Germany

Abstract

The paper investigates the feasibility of achieving uniform high-power volume heating for a fusion reactor concept employing a mixed fuel composition involving pBDT. The realm of mixed fuel fusion concepts remains relatively unexplored. The pursuit of uniform high-power volume heating presents a technological challenge, yet it bears ramifications for fusion reactor designs. In this study, we introduce the proposition of employing embedded nano-structures that represent structured foams. These structured foams interact with short-pulse lasers, thereby achieving ultra-high power volume heating both within the fuel and the adjacent hohlraums. Notably, structured foams exhibit superior efficiency compared to unstructured foams, plasma or surfaces when it comes to absorbing high-power, short-pulse lasers. The suggested incorporation of these embedded structured foams interacting with an array of ultra-short laser pulses offers a high laser absorption power density, along with meticulous control over energy and power distribution within the fuel, both in spatial and temporal dimensions. This holds the potential for the realization of fusion reactors characterized by straight-forward designs and low complexity, where $Q_F \approx Q_T > 1$ is expected for the fuel and target gains. Depending on the fuel composition they can be strong neutron sources.

Keywords: short-pulse ignition, nuclear fusion, embedded nano-structured acceleration, advanced laser arrays.

Contents

1	Introduction	1
2	Revisiting the burn fraction	3
3	Lower threshold for the density - range product	4
4	Aspects of in-situ fusion energy feedback	5
5	Fusion yield including in-situ energy feedback	6
6	Fuel heating by structured foams	7
7	Conclusions	8
8	Acknowledgements	9

1. Introduction

The indirect drive ICF approach to nuclear fusion has recently achieved a milestone at LLNL [1, 2, 3, 4, 5, 6, 7, 8, 9] demonstrating the principal viability of inertial confinement fusion for energy production. However, the implementation of the ICF concept at LLNL has limitations, as highlighted in [10]. This raises the question of whether there are alternative approaches to nuclear fusion that could be commercially viable.

The paper examines the feasibility of a volume-heated mixed fuel reactor using pBDT with a fusion gain $Q_F \approx Q_T > 1$. Mixed fuel fusion reactor concepts are relatively new, and their potential effectiveness is still uncertain.

In this paper, we propose a novel direct drive fast heating concept that relies on embedded nano-structured accelerators within the fuel, which can be considered structured foams. These nanostructures are heated using ultra-short, high-contrast laser pulses, resulting in Coulomb explosions [11]. The radiation, fast electrons, and fast ions generated by these Coulomb exploding nanostructures are then absorbed on picosecond time scales in the surrounding fuel. The heating concept resembles a combined electron and ion based fast igniter [12, 13]. This approach offers a new pathway for achieving controlled fusion reactions with enhanced efficiency and potential commercial viability. The technology has the potential to create unique density, velocity, and temperature profiles within the fuel volume without the need for fuel pre-compression. The creation of specific density, velocity, and temperature profiles are known to be a prerequisite for high gain fusion reactor designs [14?].

A comprehensive overview of the inertial confinement fusion (ICF) approach to nuclear fusion is provided in Atzeni and Meyer-ter-Vehn [15] and the references therein. The fuel yield, denoted as Q_F , is defined as the ratio of the fusion energy E_f generated to the external energy E_i deposited in the target. In the literature, as discussed in Abu-Shawareb et al. [16], the fusion gain Q_F is distinguished from the target gain $Q_T = \eta Q_F$, where η represents the energy deposition efficiency in the target. The parameter H is commonly used in the ICF context as a measure of fuel reactivity, as described in Atzeni and Meyer-ter-Vehn [15]. In this paper, kT_e is used to denote the electron temperature, while kT_i represents the ion temperature. Typically, $kT_e < kT_i$ due to radiation losses, as stated in Moreau et al. and Putvinski et al. [17, 18].

In order to determine the fusion gain Q_F , it is necessary to calculate the effective burn fraction Φ . The calculation of Φ is relatively straightforward when certain simplifying assumptions are made, such as assuming uniform electron temperature kT_e and ion temperature kT_i , and spatially homogeneous fuel in either cylindrical or spherical geometry. In the paper, we focus on cylindrical geometry and enhance the analytical model by incorporating in-situ fusion energy feedback and implementing a fuel enclosure. These improvements allow for a more accurate estimation of Φ and provide valuable insights into the performance of the system.

We propose that the energy and power deposition needs of a reactor operating at $Q_T > 1$ can be fulfilled by utilizing a uniform high power fuel heating profile without the requirement for fuel pre-compression. This can be achieved through the synergistic combination of short-pulse lasers and embedded nano-structured accelerators featuring small structure sizes. We suggest the use of materials such as boron composites, which possess the ability to chemically bind high concentrations of protons, deuterons, and tritium while maintaining a solid state. By implementing such nano-accelerators, we can effectively facilitate the desired uniform energy and power deposition within the reactor.

In cylindrical geometry and neglecting hydro-motion with the exception of fuel rarefaction, the energy E_i , the $\rho_p R$ (density times radius), and the confinement time $\Delta\tau$ necessary to achieve the desired fuel gain Q_F , as described in [15], scale in the following manner

$$\rho_p R > \frac{3 kT_i Q_F H}{\epsilon_f - 3 kT_i Q_F}, \quad (1)$$

$$\Delta\tau > \frac{1}{4u^s \rho_p} \rho_p R, \quad (2)$$

$$\frac{E_i \rho_p}{L} > \frac{3\pi kT_i}{m_p} (\rho_p R)^2. \quad (3)$$

In the given equations, ρ_p represents the mass density of protons in the fuel used for normalization, u^s denotes the sound velocity, ϵ_f represents the fusion energy without neutrons for each elementary process, R is the radius of the fuel, and L refers to the length of the fuel cylinder. When the product $kT_i Q_F H$ is large, it indicates the requirement for a high ignition energy E_i based on the underlying model described by equations (1) to (3).

The energy E_i necessary to achieve the fuel yield Q_F must be delivered to the fusion plasma within a time duration shorter than the confinement time $\Delta\tau$. According to (2) and (3) this implies

$$P_{\Delta\tau} \gg \frac{12\pi u^s kT_i}{m_p} \rho R. \quad (4)$$

Equation (4) indicates that a high product of $kT_i Q_F H$ necessitates a high deposition power. However, there is an additional power constraint that arises from the limitations imposed on the nanostructures. The nanostructures can withstand intense laser fields for only a brief period of time τ , leading to

$$P_\tau \approx \frac{E_i}{\tau} = \frac{kT_i}{m_p \tau \rho_p^2} (\rho R)^3 \gg P_{\Delta\tau}. \quad (5)$$

Therefore, it is necessary to ensure that the power supplied by the laser system, denoted as P_L , exceeds the power constraint P_τ implying $P_L > P_\tau$. Another constraint is

$$P_d \gg \frac{12\pi u^s kT_i}{m_p} \rho R, \quad (6)$$

where P_d is the energy deposition power of the electrons and ions in the fuel accelerated by the laser irradiated nano-rods and the deposition power of the associated radiation.

The scaling model presented in (1) - (3) provides limited insights into burn requirements. To fully comprehend burn requirements, it is essential to take into account fusion power gain and the transfer of power from ions to electrons, which limits radiation loss. Further details regarding this aspect are elaborated in section 4.

Mixed fuels provide a promising solution to eliminate the need for cryogenic fuel technology. By employing chemical compounds of boron that can effectively bind deuterium and tritium at room temperature in solid form, the challenges associated with cryogenic fuel handling can be overcome. The fusion performance of the fuel is closely related to the density, velocity, and temperature profiles established within it [14].

In this paper, we propose a method to achieve a uniform temperature profile in the fuel by merging multiple clusters of nano-rods, which are interlaced with the fuel, into a single reactor. This reactor is then surrounded by high-Z materials, as illustrated in Figure 1. To initiate the fusion process, the fuel is irradiated with multiple ultra-short, high contrast laser pulses. This approach enables precise control over the temperature distribution within the fuel, facilitating fast and efficient energy deposition in the fuel and enhancing fusion reactions.

Figure 1 illustrates a hypothetical cylindrical enclosed reactor configuration. The design of the reactor includes sections that are specifically optimized for laser energy deposition, which are interspersed with fuel absorber sections. The accelerator sections are composed of nano-structured fuel, serving as embedded accelerators, while the absorber sections do not possess nano-structures by default. In the figure, the laser pulses are represented as grey disks, impinging from the top.

As discussed in [11], the use of small nano-rods is motivated by their ability to deliver the required power density in the form of quasi-neutral ionic fuel flows, fast electrons, and radiation. These nano-rods play a crucial role in achieving efficient energy transfer and deposition within the reactor and to establish fusion enhancing density, velocity and temperature profiles [14] without fuel pre-compression.

As discussed in [11], nano-structures have shown excellent efficiency in absorbing short-pulse lasers, allowing for almost complete energy transfer to electrons, ions, and radiation. The laser-accelerated ions, electrons, and radiation can generate sufficiently high values of kT_e and kT_i .

The deposition power of a single rod exposed to a short laser pulse can reach up to 10, GW, while the absorbed energy by a single rod is typically in the range of a few millijoules (mJ). By combining a large number of embedded rods, the integrated deposition power and absorbed energy can be increased to meet the desired levels for any given reactor parameters,

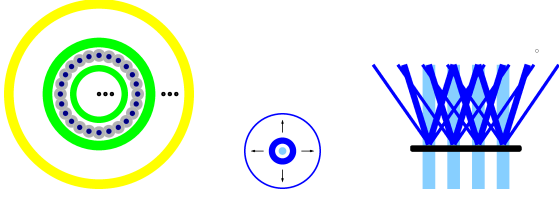


Figure 1: The left plot in Figure 1 showcases the design of a cylindrical onion shell mixed fuel reactor, which is enclosed by high-Z materials. This design aims to achieve the desired parameters of $\rho_p R$ and confinement time $\Delta\tau$. To accomplish this, the reactor incorporates acceleration layers consisting of nano-structured pBDT fuel (represented by blue and grey dots), which are alternated with higher density absorbing layers composed of unstructured pBDT fuel (depicted by green lines). Each layer can have a variable thickness ΔR . In the design, the laser pulses are incident from the top and are depicted as grey disks. The central and right plots illustrate the Coulomb explosion of a cluster of embedded nano-rods. In the right plot, the short-pulse laser is represented by the black bar, while the accelerated fuel ions are depicted by the dark blue bars. It is important to note that each rod in the cluster has the capability to absorb approximately 10 mJ of energy and deliver a laser deposition power of up to 10.0 GW.

without triggering optical instabilities. The energy deposition achieved through arrays of short laser pulses and small-sized nano-structures enables the provision of the necessary power densities for high-efficiency (η) reactor designs without the requirement for fuel pre-compression.

The paper is organized as follows. Section 2 revisits the burn fraction Φ and its significance. Section 3 focuses on the investigation of scaling relations for mixed fuel. In section 4, we delve into the discussion of in-situ fusion energy feedback. Finally, in section 7, we provide a summary of our findings and draw conclusions based on the results obtained.

2. Revisiting the burn fraction

As discussed in [19] the elementary burn fraction ϕ in the equal density limit of fuels n_k and n_l on a microscopic level is

$$\phi_{kl} = \frac{\Delta n_k}{n_k} \approx \frac{n_l \sigma_{R0}^{kl} \mathcal{R}}{1 + n_l \sigma_{R0}^{kl} \mathcal{R}} \quad (7)$$

with

$$\sigma_{R0}^{kl} \mathcal{R} = \int_0^{\Delta\tau} d\tau u_{kl}(\tau) \sigma_R^{kl}(u_{kl}(\tau)), \quad (8)$$

where σ_{R0} is the effective cross section of the reactive fluids k and l and Δt is the effective resistive stopping time. The detailed calculation of (7) and (8) requires advanced fluid kinetic simulations as is outlined in [11].

We briefly revisit the ICF paradigm in our study. We propose that by depositing short-pulse laser energy into the nano-rods of the reactor, efficient and rapid fuel heating can be achieved, as depicted in Fig. 1. If a sufficiently long confinement time $\Delta\tau$ can be established, the ions can be heated to the critical temperature kT_i , while the electrons can reach the temperature kT_e in a fraction of the latter time.

Under these assumptions, considering Maxwellian distributions of electrons and ions with uniform temperatures kT_e and

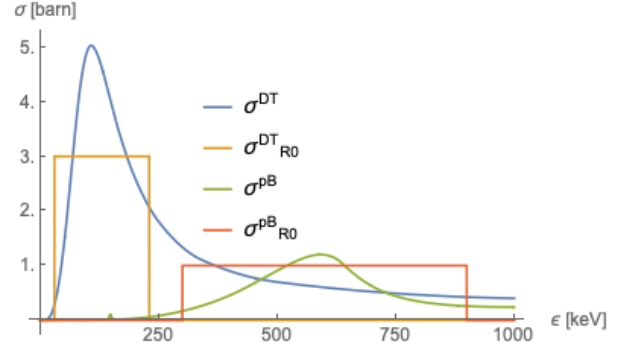


Figure 2: The cross sections σ^{DT} and σ^{pB} as functions of energy are illustrated. The yellow and purple shading highlights the piecewise constant approximations of the cross sections σ^{DT} and σ^{pB} . In the present analysis, the approximate cross sections σ_{R0}^{DT} and σ_{R0}^{pB} used are the piecewise constant approximations.

kT_i , and neglecting hydro-motion, we can calculate the reactivity

$$\sigma_{R0}^{kl} \mathcal{R} \approx \Delta\tau u_{kl} \sigma_{R0}^{kl}, \quad (9)$$

where the resistive range \mathcal{R} has been replaced by the fuel radius R in the assumed cylindrical geometry. The emergence of the radius $R \gg \mathcal{R}$ is associated with the confinement time $\Delta\tau$, which is primarily limited by fluid rarefaction at leading order, approximated by

$$\Delta\tau \approx \frac{R}{4u^s}, \quad u^s > \sqrt{\frac{3kT_Z}{m_Z}}. \quad (10)$$

Here, m_Z is an effective mass intended to account for the effective inertia of the fuel enclosure and kT_z is the effective temperature of the latter. The parameter u^s is an effective sound velocity based on the enclosure temperature kT_Z and m_Z . The burn fraction Φ in the context is

$$\Phi_{kl} \approx \frac{\rho_p R}{H_{kl} + \rho_p R} \quad (11)$$

with

$$H_{kl}(kT_i, u^s) \approx \frac{4m_p u^s}{\sigma_{R0}^{kl} u_{kl}}, \quad (12)$$

where H is normalized to the proton mass m_p without loss of generality. The σu required in (12) is approximated as follows

$$\begin{aligned} & (u_{kl} \sigma_R^{kl})(kT_i) \\ & \approx \sqrt{\frac{8kT_i}{\pi m_{kl}}} \sum_{i=1}^N \sigma_{2i-1}^{kl} \left[\left(1 + \frac{\epsilon_{2i-1}^{kl}}{kT_i} \right) e^{-\frac{\epsilon_{2i-1}^{kl}}{kT_i}} \right. \\ & \quad \left. - \left(1 + \frac{\epsilon_{2i}^{kl}}{kT_i} \right) e^{-\frac{\epsilon_{2i}^{kl}}{kT_i}} \right], \end{aligned} \quad (13)$$

where

$$m_{kl} = \frac{m_k m_l}{m_k + m_l}, \quad (14)$$

$$\sigma_R^{kl}(\epsilon) \geq \begin{cases} \sigma_{2i-1}^{kl}, & \epsilon_{2i-1}^{kl} \leq \epsilon \leq \epsilon_{2i}^{kl} \\ 0, & \text{else} \end{cases} \quad (15)$$

for $i = 1, 2, 3, \dots$ as is illustrated by the piecewise constant functions σ_{2i-1}^{DT} and σ_{2i-1}^{pB} in Fig. 2 for the fuels DT and pB. The parameters m_k and m_l are the masses of particles $k, l = \text{pBDT}$.

It is important to highlight that the replacement of \mathcal{R} with R in the hydrodynamic context is a result of thermal quasi-equilibrium. This thermal equilibrium is necessary because Coulomb collisions occur much more frequently than fusion collisions. While Coulomb collisions are still abundant in thermal equilibrium, they do not significantly alter hydrodynamic parameters on hydro timescale as soon as the latter has been reached. By establishing long confinement times for the heated fuel by technological means, which is typically in a rare fusion state, there is a possibility for fusion events to become more abundant, potentially leading to sufficient fusion gain. On the other hand, non-equilibrium fuels tend to dissipate their energy into collisional degrees of freedom, which suppresses fusion yield. In a broader context, this implies that high gain beam fusion is not feasible but may be useful for fusion reactor designs that are not intended for energy production.

3. Lower threshold for the density - range product

The understanding of the potential of mixed fuels to generate fusion energy is still incomplete. Additionally, the proposed direct drive fast heating technology opens up the possibility of achieving uniformly heated fuel volumes without fuel pre-compression. More advanced initial density, velocity, and temperature profiles may play a crucial role in achieving high gain targets, as highlighted in Kidder et al. [14].

Therefore, it is crucial to establish lower thresholds for the density-range products of potential fuel mixtures for the fuel gains Q_F at a given temperatures kT_e and kT_i . The density-range product depends on various parameters, including ϵ_f , Q_f , H , and kT_i , as expressed in equations (1) - (3). In the context of mixed fuels, these equations need to be generalized.

Let's consider a fuel mixture of pBDT with the number densities n_p, n_B, n_D , and n_T , where n_p represents the proton density, n_B represents the boron density, n_D represents the deuterium density, and n_T represents the tritium density. Utilizing the ideal gas equation of state and the reactive rate equations, we obtain

$$\frac{dn_p}{dt} \approx -n_p n_B u_{pB} \sigma_R^{pB}, \quad (16)$$

$$\frac{dn_D}{dt} \approx -n_D n_T u_{DT} \sigma_R^{DT}, \quad (17)$$

where the thermal reactivities are given by (13) and

$$E_i \approx \frac{3\pi L kT_i}{2\rho_p^2} (n_p + n_B + n_D + n_T) (\rho_p R)^2, \quad (18)$$

$$E_f \approx \frac{\pi L \epsilon_f^{DT}}{m_p \rho_p} \frac{(\rho_p R)^3}{H_{DT}(kT_i, u^s) + \rho_p R} + \frac{\pi L \epsilon_f^{pB}}{m_p \rho_p} \frac{(\rho_p R)^3}{H_{pB}(kT_i, u^s) + \rho_p R}, \quad (19)$$

where E_i is the initial energy in the reactor and the fusion energy is E_f . The parameters H_{DT} and H_{pB} can be obtained from (12).

The fuel yield Q_F is

$$Q_F = A_1 \frac{\rho_p R}{H_{DT}(kT_i, u^s) + \rho_p R} + A_2 \frac{\rho_p R}{H_{pB}(kT_i, u^s) + \rho_p R}, \quad (20)$$

where

$$A_1 = \frac{2 \epsilon_f^{DT} n_D}{3 kT_i (n_p + n_D + n_T + n_B)} \quad (21)$$

$$A_2 = \frac{2 \epsilon_f^{pB} n_p}{3 kT_i (n_p + n_D + n_T + n_B)}. \quad (22)$$

We introduce

$$H_1 = H_{DT}(kT_i, u^s), \quad H_2 = H_{pB}(kT_i, u^s) \quad (23)$$

and obtain for the lower limit of $\rho_p R$ required to reach the fuel yield Q_F at the temperatures kT_e and kT_i

$$\rho_p R \geq \frac{(H_1 + H_2) Q_F - (A_1 H_2 + A_2 H_1)}{2(A_1 + A_2 - Q_F)} + \sqrt{\frac{H_1 H_2 Q_F}{A_1 + A_2 - Q_F} + \left(\frac{(H_1 + H_2) Q_F - (A_1 H_2 + A_2 H_1)}{2(A_1 + A_2 - Q_F)} \right)^2} \quad (24)$$

where

$$Q_F \leq A_1 + A_2. \quad (25)$$

The scaled ignition energy $E_i \rho_p / L$ is obtained by plugging (24) into (18). The scalings of $E_i \rho_p / L$ and $\rho_p R$ for $Q_F = 1.0$ with reactor temperature kT_i according (18) and (24) are illustrated in Figs. 3 and 4 for two different effective sound velocities obtained for $m_Z = m_B$ and $m_Z = 16 m_B$, where m_B is the boron mass.

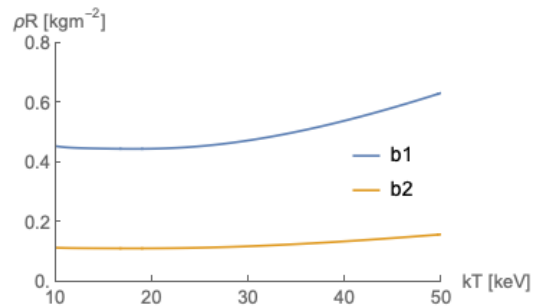


Figure 3: $\rho_p R$ for $Q_F = 1.0$ with b_1 : $n_p = n_D = n_T = n_B = 1.5 \cdot 10^{29} \text{ m}^{-3}$, $u^s = \sqrt{3 kT_i / m_B}$, and b_2 : $n_p = n_D = n_T = n_B = 1.5 \cdot 10^{29} \text{ m}^{-3}$, $u^s = \sqrt{3 kT_i / 16 m_B}$.

Other energies E_i required for fuel yields $Q_F \neq 1$ as functions of kT_i can be obtained from the $Q_F = 1.0$ case by rescaling the curves in Figs. 3 and 4 with the help of (18) and (24) and adapting the number density fractions as required.

It is evident from Figs. 3 and 4 that mixed fuel reactor concepts neglecting in-situ fusion energy feedback and measures improving confinement require unsustainably large E_i for

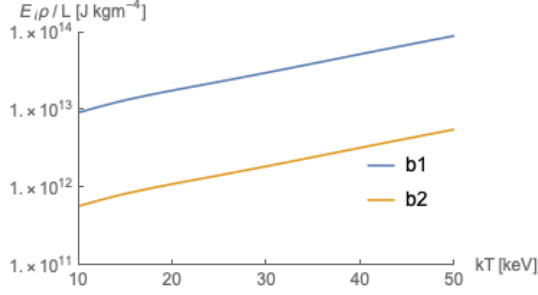


Figure 4: $E_i \rho_p / L$ for $Q_F = 1.0$ with b_1 : $n_p = n_D = n_T = n_B = 1.5 \cdot 10^{29} \text{ m}^{-3}$, $u^s = \sqrt{3kT_i/m_B}$, and b_2 : $n_p = n_D = n_T = n_B = 1.5 \cdot 10^{29} \text{ m}^{-3}$, $u^s = \sqrt{3kT_i/16m_B}$.

$Q_F \gg 1$ without fuel compression. Since we are not interested in high gain concepts in the present paper, it is obvious that confinement has to be improved implying larger effective mass m_e and fusion energy has to be fed back into the fuel.

We analyse aspects of in-situ fusion energy feedback in section 4.

4. Aspects of in-situ fusion energy feedback

In this section, we investigate the influence of in-situ fusion energy feedback on the scaled parameter $E_i \rho_p / L$. Our analysis focuses on determining the necessary electron temperature kT_e and ion temperature kT_i for achieving burn through a simple numerical model. It is important to note that we plan to enhance this model in future papers.

We first analyze the frequency integrated normalized electronic radiation power density in a plasma, which is approximated by [20]

$$\frac{P_r}{\rho_p^2} \approx \frac{16}{3\hbar m_p^2} \left(\frac{e^2}{4\pi\epsilon_0} \right)^3 \frac{\sqrt{kT_e} G}{n_p^2 (m_e c^2)^{3/2}} \times \sum_{l=D,T,p,B,\alpha} Z_l^2 n_l n_e, \quad (26)$$

where $G > 1$ is assumed and can be adapted if necessary. Next, we need the effective normalized fusion power density P_f , which is approximated as

$$\frac{P_f}{\rho_p^2} \approx a \epsilon_f^{DT} \frac{n_D n_T}{m_p^2 n_p^2} u_{DT} \sigma_{R0}^{DT} + a \epsilon_f^{pB} \frac{n_p n_B}{m_p^2 n_p^2} u_{pB} \sigma_{R0}^{pB}, \quad (27)$$

where the $a \epsilon$ in (27) with $0 \leq a < 1$ only account for the fusion energy deposited in the fuel. This implies that the energies of the fusion neutrons are neglected for the deposition of fusion energy in the fuel. The averaged reactivity $\sigma_{R0} \mu$ is given by (13). One obvious requirement for burn is

$$\frac{P_f}{\rho_p^2} \geq \frac{P_r}{\rho_p^2} \quad (28)$$

implying an upper limit for the electron temperature kT_e according to (26), at which P_r / ρ_p^2 exceeds P_f / ρ_p^2 .

We make the assumption that the transfer of energy from ions to electrons is the sole mechanism for electron energy gain in the reactor. Therefore, it is necessary to determine the rate of energy transfer from ions to electrons. Based on the work of Moreau and Spitzer [17, 21], the power transfer normalized by density from ions to electrons in the case of mixed fuels can be approximated as follows

$$\frac{P_{ie}}{\rho_p^2} \approx \sum_{l=D,T,p,B,\alpha} \frac{n_l}{m_p^2 n_p^2} t_{le}^{eq} (kT_i - kT_e), \quad (29)$$

where

$$t_{le}^{eq} \approx \frac{4\pi\epsilon_0^2 m_l m_e}{Z_l^2 q_e^4 n_e \ln \Lambda(n_l, n_e)} \left(\frac{kT_i}{m_l} + \frac{kT_e}{m_e} \right)^{3/2} \quad (30)$$

are the Spitzer equilibration times, where is approximation of Maxwellian distributions for all particles is made.

To analyze the Spitzer theory of plasma heating by α -particles in more detail we introduce the temperature kT_α to distinguish the temperature of the α -particles from the general background, which is assumed to have the temperature kT . Making the simplifying assumption $kT_e = kT_i = kT$ we obtain with the help of (29) for the ratios of the energy transfer rates between α -particles and arbitrary ions i and α -particles and electrons

$$\frac{P_{ai}}{P_{ae}} = \frac{n_e m_e}{n_i m_i} \left(\frac{1 + \frac{m_\alpha kT}{m_e kT_\alpha}}{1 + \frac{m_\alpha kT}{m_i kT_\alpha}} \right)^{3/2}. \quad (31)$$

There are a few cases that can be distinguished easily

$$\frac{m_i}{m_\alpha} < \frac{kT}{kT_\alpha} \rightarrow \frac{P_{ai}}{P_{ae}} \approx \frac{n_e}{n_i} \sqrt{\frac{m_i}{m_e}} \gg 1, \quad (32)$$

$$\frac{m_i}{m_\alpha} > \frac{kT}{kT_\alpha} > \frac{m_e}{m_\alpha} \rightarrow \frac{P_{ai}}{P_{ae}} \approx \frac{n_e m_\alpha^{3/2}}{n_i m_i \sqrt{m_e}} \left(\frac{kT}{kT_\alpha} \right)^{3/2}, \quad (33)$$

$$\frac{m_e}{m_\alpha} > \frac{kT}{kT_\alpha} \rightarrow \frac{P_{ai}}{P_{ae}} \approx \frac{n_e m_e}{n_i m_i} \ll 1. \quad (34)$$

For $kT \gg kT_\alpha$, see (34), the power transfer from α -particles into ions is much larger than the power transfer from α -particles into electrons. For $kT \ll kT_\alpha$ predominantly the electrons are heated by the α -particles. There is, however, a limit to electron heating by α -particles or ions in general. According to (29) ions cannot heat electrons as soon as $kT_e > kT_i$ holds.

To gain a comprehensive understanding of the limitations associated with the energy deposition caused by α particles and other ions in a fusion plasma, it is insufficient to focus solely on the relative heating power transferred to electrons and ions in the background plasma at an ambient temperature of kT . It is crucial to estimate the range of these particles and their total energy deposition capacity within the plasma. For information on α -particle stopping power models for DT, refer to the discussion found in [22]. A more general discussion of the stopping power exerted on ions in partially ionized matter and hot plasma is found in [23]. From [23], we quote the stopping power exerted by free electrons with the number density n_e at

the temperature kT_e on a single ion and obtain the following equations of motion

$$\frac{dr_i}{dt} = v_i, \quad (35)$$

$$\frac{dv_i}{dt} \approx -S_{fe}, \quad (36)$$

where r_i is the ion position and v_i its velocity and

$$S_{fe} \approx \frac{Z_i^2 e^4 n_e G(x_e)}{4\pi\epsilon_0^2 m_{ei} m_i v_i^2} \ln \Lambda_{fe}, \quad (37)$$

$$G(x_e) \approx \frac{2}{\sqrt{\pi}} \left(\int_0^{x_e} dt e^{-t^2} - x_e e^{-x_e^2} \right), \quad (38)$$

$$x_e \approx \sqrt{\frac{m_e v_i^2}{2kT_e}}, \quad (39)$$

$$m_{ei} = \frac{m_e m_i}{m_e + m_i}. \quad (40)$$

The parameter m_i is the ion mass and Z_i the ion charge number. The electron density n_e depends on the ionic background.

Figures 5 and 6 illustrate the range and velocity of various ions with an initial energies of $\epsilon_i = 3.5$, MeV in a pBDT mixed fuel background at $kT_e = 20$, keV. It is evident that for fuel radii ranging from $R = 1 - 2$ mm, significant fractions of the energies of the ions from the embedded accelerators and of the α particles can be deposited in the plasma. The range of the α particles implies that the scaled parameter $E_i \rho_p / L$ will significantly decrease by incorporating in-situ fusion energy feedback, as compared to Fig. 4.

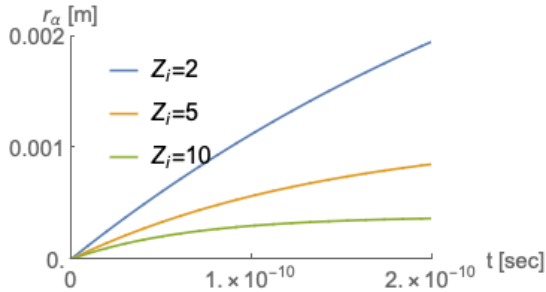


Figure 5: Ranges of various ions including α -particles as functions of time with initial energy $\epsilon_i = 3.5$ MeV in the pBDT fuel mix at $kT_e = 20$ keV with the number densities $0.6 n_p = 0.6 n_D = 0.6 n_T = n_B$, where $\rho_p \approx 300 \text{ kgm}^{-3}$.

We determine lower temperature thresholds, specifically $kT_e < kT_i$, at which the deposited normalized fusion power surpasses the normalized power transfer from ions to electrons by equating

$$\frac{P_f}{\rho_p^2} = \frac{P_{ie}}{\rho_p^2} = \frac{P_r}{\rho_p^2}. \quad (41)$$

It is important to note that this temperature threshold also serves as the upper limit for the normalized radiation power.

Figure 7 illustrates that for $0.6 n_p = 0.6 n_D = 0.6 n_T = n_B = 0.5 \cdot 10^{29} \text{ m}^{-3}$, equations (41) are satisfied if $kT_e \approx 0.73 kT_i$ and $kT_i \approx 18$ keV, assuming that the total energy of the fusion

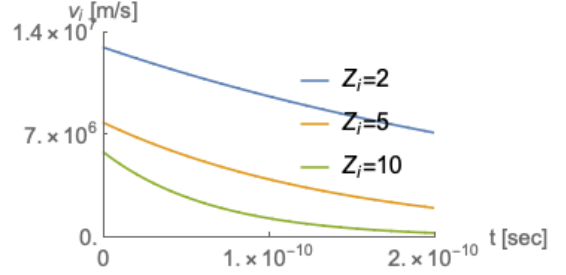


Figure 6: Velocities of various ions including α -particles as functions of time with initial energy $\epsilon_i = 3.5$ MeV in the pBDT fuel mix at $kT_e = 20$ keV with the number densities $0.6 n_p = 0.6 n_D = 0.6 n_T = n_B$, where $\rho_p \approx 300 \text{ kgm}^{-3}$.

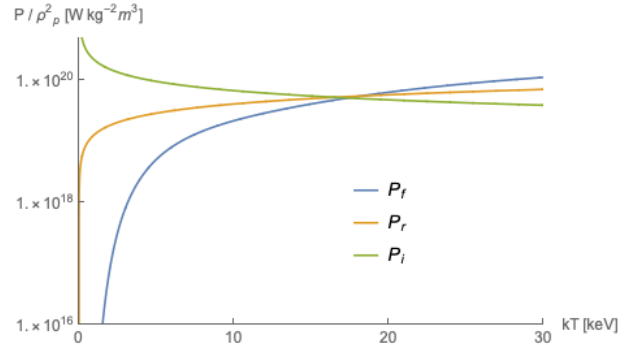


Figure 7: Scaled fusion, radiation, and transfer powers for the mixed fuel consisting of pBDT. It holds $P_f/\rho_p^2 = P_r/\rho_p^2 = P_{ie}/\rho_p^2$ at $kT_i \approx 18$ keV and $kT_e \approx 0.73 kT_i$ for $G = 1$. The number densities are $0.6 n_p = 0.6 n_D = 0.6 n_T = n_B = 0.5 \cdot 10^{29} \text{ m}^{-3}$ and $n_e = \sum_{k=p,D,T} Z_k n_k$.

α -particles is deposited in the fuel and radiation losses are described by (26) with $G = 1$.

Therefore, if the embedded accelerator technology is capable of heating fuel ions to $kT_i > 18$ keV for the fuel number densities in pBDT within a fraction of the confinement time, implying $\Delta\tau \gg t_{ij}^{eq}$, the ion temperature kT_i can continue to increase up to an upper limit unless there are additional loss processes not considered in this section.

5. Fusion yield including in-situ energy feedback

In this section, we analyze the influence of in-situ fusion energy feedback and enhanced inertia on the fusion yield of the mixed fuel pBDT. To account for the highly nonlinear impact of in-situ fusion energy feedback on the ambient fusion plasma, we employ a simple numerical model that allows radiation to freely exit the reactor. This approach facilitates the investigation of the effects of feedback and enhanced inertia on the fusion yield.

By adjusting the available fusion power in the plasma aP_f , we can account for the incomplete deposition of the energy carried by the α -particles in the fuel. To model the influence of a high- Z enclosure, as illustrated in Fig 1, we introduce the effective temperature $kT_Z = c kT_i$ with $0 \leq c < 1$ and the effective fuel mass m_Z . These parameters modify fluid rarefaction in the system. Meanwhile, the fuel temperatures are given by

$kT_e = b, kT_i$, where $0 < b \leq 1$, as derived from equations (32) - (41).

Assuming known densities n_p , n_D , n_T , and n_B , and the applicability of ideal equations of state, we consider an initial energy in the fuel of $E_f^0 = E_i$ and an initial electron temperature of kT_e^0 . From these conditions, we derive the initial ion temperature kT_i^0 as follows

$$kT_i^0 = \frac{2 \left(E_i^0 - \frac{3}{2} \pi L R^2 n_e k T_e^0 \right)}{3 \pi L R^2 (n_p + n_D + n_T + n_B)}. \quad (42)$$

Next, we make the assumption that the electron temperature kT_e rapidly decreases, resulting in $kT_e = b, kT_i$ with $0 \leq b < 1$. Our reactor configuration is enclosed within high-Z materials, as illustrated in Figure 1. To approximate hydrodynamic effects, we employ an effective fluid rarefaction model using the effective temperature kT_Z and the effective mass m_Z . In this model, we neglect fuel depletion due to reactions. With these considerations, we utilize the simplified model below to estimate the fusion yield Q_F incorporating in-situ fusion energy feedback into our analysis.

We set $\Delta t = 10^{-12}$ s, $m_Z = 2.7 \cdot 10^{-25}$ kg, $a = 0.3$, $b = 0.73$, $c = 0.1$, $\rho_{DT} = 500 \text{ kgm}^{-3}$, $\rho_{pB} = 800 \text{ kgm}^{-3}$, $0.6 n_p = 0.6 n_D = 0.6 n_T = n_B$, $kT_e = 20 \text{ keV}$, and $R = L = 1.0 \text{ mm}$ and iterate

$$t^n = t^{n-1} + \Delta t, \quad (43)$$

$$kT_i^n = \frac{2 \left(E_d^n - \frac{3}{2} \pi L R^2 n_e k T_e^n \right)}{3 \pi L R^2 (n_p + n_D + n_T + n_B)},$$

$$kT_e^n = b kT_i^n$$

$$kT_Z^n = c kT_i^n,$$

$$u^n = \sqrt{\frac{3 kT_Z^n}{m_Z}},$$

$$\Delta \tau^n = \frac{R}{4 u^n},$$

$$E_d^n = E_d^{n-1} + \pi L R^2 \Delta t \left[a P_f(kT_i^n) - P_{ie}(kT_i^n, kT_e^n) \right],$$

where $\Delta \tau^n \gg t_{ij}^{eq,n}$ is assumed and

$$E_f^n = E_f^{n-1} + \pi L R^2 \Delta t P_f(kT_i^n),$$

$$E_\alpha^n = E_\alpha^{n-1} + \pi L R^2 \Delta t P_f(kT_i^n),$$

$$E_n^n = E_n^{n-1} + \frac{14.1}{3.5} \pi L R^2 (1 - a) \Delta t P_f(kT_i^n),$$

$$E_r^n = E_r^{n-1} + \pi L R^2 \Delta t P_{ie}(kT_i^n),$$

$$Q_F^n = \frac{E_f^n}{E_i}.$$

The term Q_F^n represents the fuel yield without neutrons at time t^n . The parameters E_d , E_f , E_n , E_r , and E_α correspond to the integrated fusion energy deposition in the fuel ions, the integrated fusion energy, the integrated neutron energy, the integrated emitted radiation energy, and the emitted α -particle energy at time t^n , respectively. The parameter a denotes the fraction of the energy of the α -particles that is deposited in the fuel.

This value is determined using the stopping power of the α -particles in a plasma with temperatures $kT_e^n = b, kT_i^n$. The parameter b characterizes the degree of electron heating in the fuel, while the parameters c and m_Z control the effective confinement of the latter.

The fusion power P_f and the power transfer from ions to electrons P_{ie} are given by equations (27) and (29), respectively. The conditions $\Delta \tau^n \gg t_{ij}^{eq,n}$ indicate that the energy equilibration time between ions and electrons and between ions within the fuel is much shorter than the confinement time $\Delta \tau^n$. The loop in equation (43) is terminated when $t^n > \Delta \tau^n$.

Figures 8, 9, and 10 show the fuel yield, the fuel temperatures kT_e and kT_i , and various ion energies and the neutron energy as functions of time in the reactor. The neutrons carry the bulk of the generated fusion energy in the reactor.

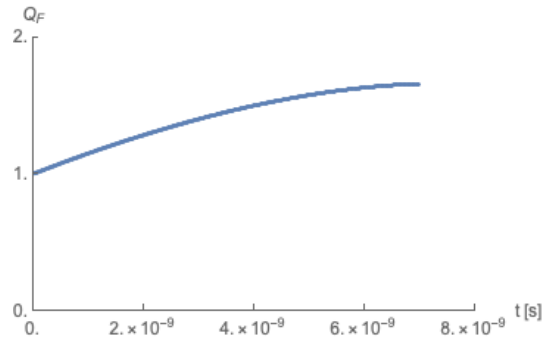


Figure 8: The fuel yield Q_F^n is a time-dependent quantity that neglects the contribution of neutrons. The parameters used in this context are $0.6 n_p = 0.6 n_D = 0.6 n_T = n_B$, where $\rho_{DT} = 500 \text{ kgm}^{-3}$ and $\rho_{pB} = 800 \text{ kgm}^{-3}$. The initial temperatures are set to $kT_i^0 = 20 \text{ keV}$ and $kT_e^0 = 0.73 kT_i^0$.

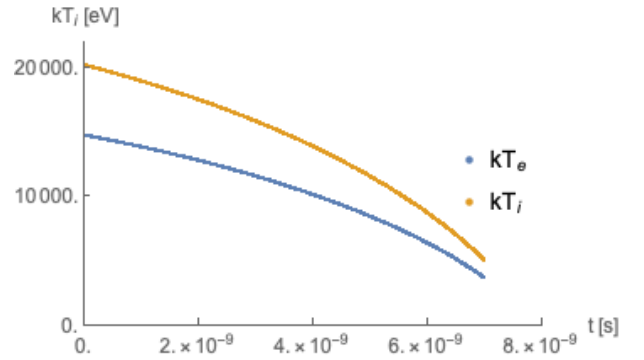


Figure 9: Temperatures kT_e^n and kT_i^n as functions of time. The parameters are $0.6 n_p = 0.6 n_D = 0.6 n_T = n_B$, where $\rho_{DT} = 500 \text{ kgm}^{-3}$ and $\rho_{pB} = 800 \text{ kgm}^{-3}$. The initial temperatures are $kT_i^0 = 20 \text{ keV}$ and $kT_e^0 = 0.73 kT_i^0$.

6. Fuel heating by structured foams

The arrangement of the direct drive fast fuel heating concept for the proposed low-gain fusion reactor can be modeled using the effective rod concept, as detailed in the work by Ruhl et

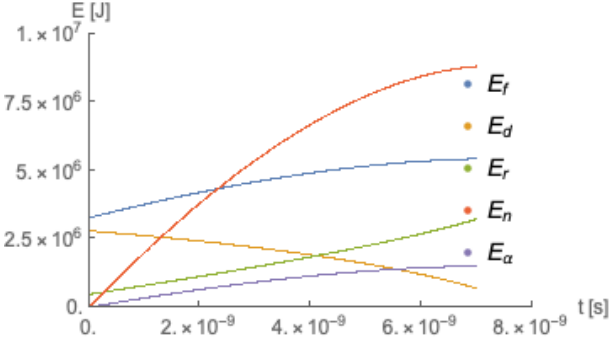


Figure 10: Fusion energies as functions of time, where E_f^n , E_d^n , E_r^n , E_n^n , and E_α^n are the integrated fusion, ion deposition, radiation loss, neutron loss, and exiting α -particle energies as functions of time. The other parameters are $0.6n_p = 0.6n_D = 0.6n_T = n_B$, where $\rho_{DT} = 500 \text{ kgm}^{-3}$ and $\rho_{pB} = 800 \text{ kgm}^{-3}$. The initial temperatures are $kT_i^0 = 20 \text{ keV}$ and $kT_e^0 = 0.73 \text{ keV}$.

al. [24]. According to the discussions presented in this reference, the effective rod model can be envisioned as a structured foam, suitable for operation under the conditions of a single effective rod limit. Structured foams exhibit superior laser energy and power absorption capabilities compared to the unstructured foams, the homogeneous plasma or the empty hohlraums.

In this context, an effective single rod demonstrates the ability to efficiently absorb laser energy at a consistent rate per surface area A_r and per unit length of laser propagation. As elucidated in Ruhl et al. [24], the extent of laser energy and power absorption is contingent upon factors such as the radius of the rod, the material it is composed of, and the spacing $\sqrt{A_r}$ between neighboring rods called the pitch.

In simulations conducted with a specific configuration featuring a rod diameter of 30 nm and a pitch $\sqrt{A_r} \approx 500 \text{ nm}$, as outlined in [24], the calculated absorption power density of a single effective rod is approximately

$$\epsilon_r \approx 1.2 \cdot 10^{-2} \frac{\text{J}}{\mu\text{m}^3}. \quad (44)$$

We note that structured foams can be placed and oriented in any desired way in a given volume.

For the sake of simplicity, we adopt a cylindrical geometry in our considerations. We make the assumption that the nano-rods are arranged radially, ensuring even distribution across the area defined by the radius R_r and the radial width ΔR_r . Additionally, these rods are assumed to be aligned along the cylinder axis and possess a uniform length denoted as ΔL_r .

Under the assumptions made the total energy, denoted as E , which the structured foam comprised of these rods can potentially absorb, is approximately determined by ϵ_r , R_r , ΔR_r , and ΔL_r . We obtain

$$\begin{aligned} E &\approx 2\pi \epsilon_r R_r \Delta R_r \Delta L_r \\ &= 7.53 \cdot 10^{-2} R_r \Delta R_r \Delta L_r \frac{\text{J}}{\mu\text{m}^3}. \end{aligned} \quad (45)$$

With the help of (45) the required radius R_r is approximately

given by

$$\begin{aligned} R_r &\approx \frac{E}{2\pi \epsilon_r \Delta R_r \Delta L_r} \\ &\approx 13.2 \frac{E}{\Delta R_r \Delta L_r} \frac{\mu\text{m}^3}{\text{J}} \approx 2000 \mu\text{m}, \end{aligned} \quad (46)$$

where it has been assumed that $\Delta R_r \approx 500 \mu\text{m}$, $\Delta L_r \approx 30 \mu\text{m}$, and $E \approx 4 \cdot 10^6 \text{ J}$ hold. The number of rods N needed to absorb the laser energy E given ϵ_r , R_r , ΔR_r , and A_r is approximately

$$N \approx \frac{2\pi R_r \Delta R_r}{A_r} = \frac{E}{\epsilon_r \Delta L_r A_r} \approx 5 \cdot 10^7, \quad (47)$$

where $E \approx 4 \cdot 10^6 \text{ J}$, $A_r \approx 0.25 \mu\text{m}^2$, and $\Delta L_r = 30 \mu\text{m}$ have been taken. Since the single effective rod can only withstand the laser radiation for the time τ the required laser power P_L is approximately

$$P_L \approx \frac{E}{\tau} \approx 8 \cdot 10^{19} \text{ W}, \quad (48)$$

where $E \approx 4 \cdot 10^6 \text{ J}$ and $\tau \approx 50 \text{ fs}$ have been assumed. The required laser power P_L can be delivered by independent beamlines. If a single beamline is capable of delivering 1 kJ and $2 \cdot 10^{16} \text{ W}$ about 4000 independent beamlines are required.

The uniformity of laser energy deposition in the fuel is contingent upon how the structured foams are distributed within the high-Z hohlraum. It's important to emphasize that the option exists to physically isolate the structured foams from the fuel, if necessary, to mitigate the introduction of high-Z contaminants into the fuel, while the structured foams can also be embedded into the fuel if required.

It's worth highlighting that structured foams can be deliberately designed to effectively convert the majority of incident laser energy into electrons, ions, and radiation thereby generating significantly elevated radiation energy densities. The subsequent reasoning serves to illustrate this point.

In the absence of structured foams, achieving adequate radiation homogeneity within a hohlraum necessitates multiple low intensity reflections of laser radiation distributed over a larger area. Consequently, the volume of such a hohlraum must be considerably larger than the fuel pellet volume and in addition can only be irradiated over an extended period of time. Hence, the energy density in such a hohlraum is low. This scenario contrasts with the case of structured foams filling a volume, wherein incident laser radiation can be absorbed over the much smaller volume $R_r \Delta R_r \Delta L_r$ in a fraction of the time leading to much higher energy densities that are available almost instantaneously.

This distinctive characteristic translates to the fact that for structured foams, at any given radiation temperature, the requisite hohlraum volume is roughly equivalent to the fuel volume. This, in turn, results in minimal wastage of laser energy for filling expansive hohlraum volumes with surplus radiation energy. In addition, the laser energy is deployed almost instantly.

7. Conclusions

In this paper, we introduce a novel direct drive fast heating technology for reactive mixed pBDT fuels and simple low gain

fusion reactor designs based on them, which can reach $Q_T > 1$ with MJ level heating energy. Simple low gain fusion reactors might be building blocks of secondary applications. Specifically, they are useful for the development of required laser and target technologies and are powerful neutron sources.

The heating technology involves the use of nano-structured accelerators embedded within the fuel powered by ultra-short high contrast laser pulses. The embedded nano-accelerators represent embedded structured foams. These foams are capable of absorbing MJ level laser energy on sub-picosecond time scales, while the energy deposition in the mixed fuel requires a couple of picoseconds. The structured foams in combination with modern short pulse lasers enable ultra-powerful ultra-fast direct drive fuel heating avoiding parametric instabilities. The structured foams can be used for constructing a new class of ultra-efficient ultra-high energy density hohlraums.

By employing a simple numerical model, the impact of in-situ fusion energy feedback and effective fuel confinement can be analyzed. In-situ fusion energy feedback significantly reduces the required scaled initial energy $E_i \rho_p / L$. According to Fig. 10 the numerical model predicts that an initial energy of approximately 3.4 MJ is sufficient to achieve a fuel yield $Q_F > 1$ for the simple reactor concept discussed here. It is important to note that the numerical model can be adapted to fit more sophisticated simulations with a community code with the help the effective parameters a, b, c for a given set of initial temperatures kT_e and kT_i , and initial density-range product $\rho_p R$, and relative fractions of the fuel number densities involved.

It is important to note that energy production requires a target gain $Q_T = \eta Q_F \approx 30 - 50$, as discussed in [25], which is much larger than the one predicted for the parameters investigated in the present paper.

8. Acknowledgements

The present work has been motivated and funded by Marvel Fusion GmbH.

References

- [1] M. Banks, Significant step towards break-even target, *Physics World* 34 (10) (2021) 11ii.
- [2] A. B. Zylstra, et al., [Burning plasma achieved in inertial fusion](https://doi.org/10.1038/s41586-021-04281-w), *Nature* 601 (2022) 542–548. doi:10.1038/s41586-021-04281-w. URL <https://doi.org/10.1038/s41586-021-04281-w>
- [3] H. Abu-Shawareb, et al., [Lawson criterion for ignition exceeded in an inertial fusion experiment](https://link.aps.org/doi/10.1103/PhysRevLett.129.075001), *Phys. Rev. Lett.* 129 (2022) 075001. doi:10.1103/PhysRevLett.129.075001. URL <https://link.aps.org/doi/10.1103/PhysRevLett.129.075001>
- [4] A. L. Kritcher, et al., [Design of an inertial fusion experiment exceeding the lawson criterion for ignition](https://link.aps.org/doi/10.1103/PhysRevE.106.025201), *Phys. Rev. E* 106 (2022) 025201. doi:10.1103/PhysRevE.106.025201. URL <https://link.aps.org/doi/10.1103/PhysRevE.106.025201>
- [5] A. B. Zylstra, et al., [Experimental achievement and signatures of ignition at the national ignition facility](https://link.aps.org/doi/10.1103/PhysRevE.106.025202), *Phys. Rev. E* 106 (2022) 025202. doi:10.1103/PhysRevE.106.025202. URL <https://link.aps.org/doi/10.1103/PhysRevE.106.025202>
- [6] U. D. of Energy, [Doe national laboratory makes history by achieving fusion ignition](https://www.llnl.gov/news/national-ignition-facility-achieves-fusion-ignition), retrieved on Dec. 14, 2022 (Dec 2022).
- [7] B. Bishop, [National ignition facility achieves fusion ignition](https://www.llnl.gov/news/national-ignition-facility-achieves-fusion-ignition), retrieved Dec. 14, 2022 (Dec 2022). URL <https://www.llnl.gov/news/national-ignition-facility-achieves-fusion-ignition>
- [8] K. Chang, [Scientists achieve nuclear fusion breakthrough with blast of 192 lasers](https://www.nytimes.com/2022/12/13/science/nuclear-fusion-energy-breakthrough.html), retrieved Dec. 14, 2022 (Dec 2022). URL <https://www.nytimes.com/2022/12/13/science/nuclear-fusion-energy-breakthrough.html>
- [9] D. Clercy, [With historic explosion, a long sought fusion breakthrough](https://www.science.org/content/article/historic-explosion-long-sought-fusion-breakthrough), retrieved Dec. 14, 2022 (Dec 2022). URL <https://www.science.org/content/article/historic-explosion-long-sought-fusion-breakthrough>
- [10] O. Hurricane, D. Callahan, A. Kritcher, A. Zylstra, [Optimism is not a strategy: A white paper of how to give ife a fighting chance to be real](https://lasers.llnl.gov/content/assets/docs/nif-workshops/ife-workshop-2021/white-papers/hurricane-LLNL-IFE-workshop-2022.pdf) (2022). URL <https://lasers.llnl.gov/content/assets/docs/nif-workshops/ife-workshop-2021/white-papers/hurricane-LLNL-IFE-workshop-2022.pdf>
- [11] H. Ruhl, G. Korn, High current ionic flows via ultra-fast lasers for fusion applications (Dec. 2022). doi:10.48550/arXiv.2212.12941.
- [12] M. Tabak, J. Hammer, M. E. Glinsky, W. L. Kruer, S. C. Wilks, J. Woodworth, E. M. Campbell, M. D. Perry, R. J. Mason, Ignition and high gain with ultrapowerful lasers, *Physics of Plasmas* 1 (5) (1994) 1626–1634.
- [13] M. Roth, T. Cowan, M. Key, S. Hatchett, C. Brown, W. Fountain, J. Johnson, D. Pennington, R. Snavely, S. Wilks, et al., Fast ignition by intense laser-accelerated proton beams, *Physical review letters* 86 (3) (2001) 436.
- [14] R. E. Kidder, Application of lasers to the production of high-temperature and high-pressure plasma, *Nuclear Fusion* 8 (1) (1968) 3.
- [15] S. Atzeni, J. Meyer-ter Vehn, *The physics of inertial fusion: beam plasma interaction, hydrodynamics, hot dense matter*, Vol. 125, OUP Oxford and citations therein, 2004.
- [16] H. Abu-Shawareb, R. Acree, P. Adams, J. Adams, B. Addis, R. Aden, P. Adrian, B. Afeyan, M. Aggleton, L. Aghaian, et al., Lawson criterion for ignition exceeded in an inertial fusion experiment, *Physical Review Letters* 129 (7) (2022) 075001.
- [17] D. C. Moreau, Potentiality of the proton-boron fuel for controlled thermonuclear fusion, *Nuclear Fusion* 17 (1) (1977) 13.
- [18] S. Putvinski, D. Ryutov, P. Yushmanov, Fusion reactivity of the pb11 plasma revisited, *Nuclear Fusion* 59 (7) (2019) 076018.
- [19] H. Ruhl, G. Korn, [A laser-driven mixed fuel nuclear fusion micro-reactor concept](https://arxiv.org/abs/2202.03170) (Feb. 2022). doi:10.48550/arXiv.2202.03170.
- [20] G. Befki, *Radiation processes in plasmas*, Wiley series in plasma physics (1966).
- [21] L. Spitzer, *Physics of fully ionized gases*, Courier Corporation, 2006.
- [22] N. Xu, *Effects of alpha particle stopping-power models on inertial confinement fusion implosions* (2014).
- [23] M. Basko, *Stopping of fast ions in dense plasmas*, Tech. rep., Institute of Theoretical and Experimental Physics (1983).
- [24] H. Ruhl, G. Korn, [Uniform volume heating of mixed fuels within the ICF paradigm](https://arxiv.org/abs/2302.06562) (Feb. 2023). doi:10.48550/arXiv.2302.06562.
- [25] L. Perkins, et al., *And Now on to Higher Gains: Physics Platforms and Minimum Requirements for Inertial Fusion Energy, IFE Strategic Planning Workshop Kickoff*, 2021.